Carbohydrate Polymers 95 (2013) 492–500

Contents lists available at SciVerse ScienceDirect

Carbohydrate Polymers

journal homepage: www.elsevier.com/locate/carbpol

Reaction patterns of wheat starch granules substituted with an anionic propylene oxide analog (POA) revealed by confocal microscopy and 3D anaglyph imaging

Hyun-Seok Kim [a], Kerry C. Huber [b,*]

[a] Department of Food Science and Biotechnology, Andong National University, 1375 Gyeongdong-ro, Andong-si, Gyeongsangbuk-do 760-749, Republic of Korea
[b] School of Food Science, University of Idaho, P.O. Box 442312, Moscow, ID 83844-2312, USA

ARTICLE INFO

Article history:
Received 4 January 2013
Received in revised form 21 February 2013
Accepted 5 March 2013
Available online 13 March 2013

Keywords:
Wheat starch A-type granule
Chemical modification
Granular reaction pattern
Propylene oxide analog (POA)
Confocal laser scanning microscopy (CLSM)
Anaglyph 3D image

ABSTRACT

A technique was developed for investigating granular reaction patterns of anionic starch derivatives, utilizing the optical sectioning capability of reflectance confocal laser scanning microscopy in combination with 3D anaglyphic imaging (3D glasses required for visualization). The method facilitated improved visualization of internal granular reaction patterns by discarding optical sections comprising the highly-reacted external granule surface (generating 3D image constructs from sections constituting exclusively internal regions of granules) and minimizing confounding background signal associated with non-starch constituents (e.g., proteins). For wheat starch A-type granules substituted with a propylene oxide analog (POA), granular reaction patterns revealed that reagent reached the hilum region of granules through channels, and primarily entered the granule matrix via lateral diffusion from channel surfaces, producing relatively homogeneous reaction patterns. The homogeneous nature of POA granular reaction patterns was attributed to the relatively low reactivity of the reagent (rate of diffusion > rate of reaction).

1. Introduction

Starch, one of the most abundant component biomass resources in the world, is composed of two homopolymers of α-D-glucose: linear amylose and highly-branched amylopectin (Tester, Karkalas, & Qi, 2004). Within higher plants, amylose and amylopectin molecules are assembled together to form complex, ordered, semi-crystalline aggregates, referred to as granules (Zobel & Stephen, 2006). Granular starch is utilized in food and non-food applications as a thickening agent, colloidal stabilizer, gel-forming agent, water retention agent, binder, and coating and/or glazing agent (Singh, Kaur, & McCarthy, 2007; Zobel & Stephen, 2006). Nevertheless, starches in their native form exhibit inherent physical defects (e.g., poor solubility in cold water, poor shear and heat resistance, uncontrolled paste consistency, high tendency toward retrogradation) that make them non-ideal for both existing and emerging applications (BeMiller, 1997; Wurzburg, 2006). To overcome the noted inherent limitations, the majority of starch (while yet in the granular state) intended for use as a food ingredient is first chemically modified to improve and extend its physical properties in accordance with the intended application (Alexander, 1992).

Though chemically-modified starches have been extensively studied with respect to their preparation and physical properties (Gray & BeMiller, 2004, 2005; Han & BeMiller, 2005, 2006, 2007; Huber & BeMiller, 2001; Kavitha & BeMiller, 1998; Kim & Huber, 2010a; Shi & BeMiller, 2000; Woo and Seib, 1997, 2002), starch granule reactivity is still not completely understood. During reaction, it is the granule structure that ultimately dictates the accessibility of individual starch molecules to derivatizing reagents, impacting both granular and molecular reaction patterns, and thus starch properties. Nevertheless, complicating aspects of starch granule structures include: (1) variable ratios of amylose to amylopectin (e.g., waxy, partial waxy, normal, high amylose), (2) varying levels of minor non-starch components (e.g., proteins, lipids), (3) differing crystalline packing arrangements (e.g., A-type, B-type, C-type), (4) varied microstructures (e.g., pores/channels, no pores/channels), and (5) diverse shapes and sizes (BeMiller, 1997; Huber & BeMiller, 2001; Gray & BeMiller, 2004). Thus, the relationship between starch granule structure and reactivity requires further elucidation to better understand the extent to which starch modification processes/conditions can be manipulated or controlled to achieve the desired properties for food and non-food industrial applications.

Despite the noted complexity of starch granules, microstructural features such as surface pores, channels, and cavities (Huber & BeMiller, 1997), which are well elucidated in corn and

* Corresponding author. Tel.: +1 208 885 4661; fax: +1 208 885 4667.
E-mail address: huberk@uidaho.edu (K.C. Huber).

0144-8617/$ – see front matter © 2013 Elsevier Ltd. All rights reserved.
http://dx.doi.org/10.1016/j.carbpol.2013.03.023

sorghum starch granules, are known to impact starch granule reactions by facilitating access of derivatizing reagent to starch chains within the granule matrix (Huber & BeMiller, 2000, 2001; Gray & BeMiller, 2004). More recently, the presence of channel structures within wheat starch granules was verified, and the nature of these granule features was more clearly characterized (Kim & Huber, 2008). Channel structures within A-type granules of waxy and normal wheat starch are radially-oriented, penetrate to varying depths into the granule toward the hilum (i.e., cavity), and are lined/filled with protein (Kim & Huber, 2008). In preliminary experiments with a fluorescent reactive dye, channels appeared to aid passage of reagent into the granule matrix, which effect was enhanced by some degree of granule hydration/swelling and/or removal of channel-associated proteins (Kim & Huber, 2008). Though pores, channels, and cavities within wheat starch granules likely impact starch reactivity, their specific role in granule reactions has not yet been fully investigated. To date, no study has investigated granular reaction patterns within wheat starch granules derivatized with commercial modifying reagents.

Reaction within starch granules is influenced by interactions between starch granule microstructure (e.g., pores, channels, cavities) and reagent addition levels (Huber & BeMiller, 2001; Gray & BeMiller, 2004). By varying reagent addition levels, the progression of reaction within granules may provide insight into the mode of reagent flow into starch granules, which understanding may be useful for optimizing reaction conditions to achieve desired reaction patterns and/or starch properties. Starch granular reaction patterns for anionic starch derivatives may be visualized via reflectance confocal laser scanning microscopy (R-CLSM) (Gray & BeMiller, 2004), providing insight into the relative extent of reaction, as well as the distribution and locale of reaction sites, within starch granules. However, a possible limitation of this method is that it provides only a two-dimensional view of granular reaction patterns based on a single optical section from a given granule, though reagent flow into granules occurs in three dimensions.

Utilizing an anionic propylene oxide reagent analog, the objective of this study was to investigate granular reaction patterns within wheat starch A-type granules as a function of genotype (waxy versus normal), microstructure (e.g., pores, channels, cavities), and reagent addition level (low, medium, high). Further effort was devoted to development of an imaging strategy for visualization of granular reaction patterns in three dimensions (i.e., 3D anaglyph images).

2. Materials and methods

2.1. Materials

Grain of waxy (IDO630) and wild-type (Jubilee) soft wheat lines, obtained from the University of Idaho Aberdeen Research and Extension Center (Aberdeen, ID, USA), were the sources of starch used in this study. Wheat grain was milled to straight-grade flour according to AACC Approved Method 26–31 (AACC, 2000), after which starch was isolated from flours via the adapted protein-digestion scheme outlined by Kim and Huber (2008). All reagents and chemicals used in this study were of analytical grade.

2.2. Purification of wheat starch A-type granules

A purified wheat starch A-type granule fraction was recovered from isolated wheat starch through slight modification of the A- and B-type granule separation method outlined by Kim and Huber (2010b). Native starch (25 g, dry basis or d.b.) was suspended in deionized water (900 ml, containing 0.02% sodium azide) within a tall beaker (1000 ml, 7.6 cm in diameter, 18 cm depth) via constant stirring (10 min), after which larger (predominantly A-type) starch granules within the suspension were allowed to sediment (140 min, in the absence of stirring) at ambient temperature (22 °C) to the bottom of the beaker. Following the sedimentation period, the top layer of supernatant (~800 ml), containing predominantly smaller B-type granules, was discarded by careful pipetting. The resulting starch sediment (at the bottom of the beaker) was subjected to four additional sedimentation schemes as previously described (replenishment of fresh deionized water [800 ml] to the beaker, sedimentation [140 min], and removal of supernatant [~800 ml]). Starch sediment from the final sedimentation scheme was suspended in 80% (w/v) aqueous sucrose solution (180 ml) within a 250 ml centrifuge bottle (20 min) using a Wrist Action Shaker (Model 75, Burrell Co., Pittsburgh, PA, USA), after which the starch suspension was centrifuged (2000 × *g*, 3 min), and the supernatant was carefully discarded. The bottle was replenished with fresh sucrose solution (180 ml), and the aforementioned purifying procedure was repeated a total of five times. The final starch pellet obtained after the last purifying step in 80% sucrose solution was washed three times with deionized water (200 ml per wash), re-suspended in absolute ethanol, recovered on a Büchner funnel, and allowed to air-dry. Granule size distributions and purities of the final purified wheat starch A-type granules were monitored using an Accusizer model 780 with SW 788 Windows software (Particle Sizing Systems, Santa Barbara, CA, USA) as described by Geera, Nelson, Souza, and Huber (2006). The purities of obtained A-type granule fractions (>10 μm diameter) of waxy and normal wheat starches were 99.7% and 99.6% (volume or weight basis), respectively.

2.3. Modification of wheat starch granules with a propylene oxide analog (POA)

Anionic derivatives of waxy and normal starch A-type granules were produced by reaction with sodium 3-chloro-2-hydroxy-1-propanesulfonate (propylene oxide analog, POA) as outlined by Han and BeMiller (2005) and Huber and BeMiller (2001). Absolute ethanol was utilized as a swelling inhibitor, and reaction system parameters for all POA derivatives and their corresponding reaction controls are depicted in Table 1. POA reagent amounts were 2%, 6%, and 10% (starch basis or s.b.) for low, medium, and high reagent addition levels, respectively.

The appropriate level of POA reagent was dissolved in a mixture of 0.125 M NaOH, deionized water, and absolute ethanol (Table 1), followed by the addition of starch (5.0 g, d.b.) with rapid stirring. The reaction system was supplemented with an appropriate amount of 2 M NaOH in relation to the amount of incorporated reagent (1 mole POA generates 1 mole HCl) to maintain the the reaction medium pH at 11.5. The reaction mixture was incubated at 45 °C for 24 h under constant stirring, after which it was neutralized with 1.0 M HCl. After neutralization, POA starch derivatives (including reaction controls) were recovered by centrifugation (3000 × *g*, 20 min), and suspended in aqueous ethanol (50%, v/v) (Han & BeMiller, 2006) on a Wrist Action Shaker (Model 75, Burrell Co., Pittsburgh, PA, USA) for 2 h to extract unbound reagent from granules (while minimizing leaching of POA-derivatized starch molecules from granules). Derivatized starch granules were again recovered by centrifugation (3000 × *g*, 20 min). This washing procedure (beginning with the re-suspension of POA derivatives in aqueous ethanol) was repeated two more times. Washed POA starch derivatives were suspended in absolute ethanol, recovered on a Büchner funnel, and allowed to air-dry.

POA starch derivatives and reaction controls were assayed for sulfur content via inductively coupled plasma-atomic emission spectroscopy (ICP-AES) (Kim & Huber, 2010a) to determine molar substitution (MS) levels. Derivatized starch MS values, calculated

Table 1
Reaction system parameters for substitution of waxy and normal wheat starch A-type granules with a propylene oxide analog (POA).

Starch derivatives	POA (%, s.b.[a])	Reaction medium composition[b,c,d]			
		0.125 M NaOH (ml)	2.0 M NaOH (ml)	Deionized water (ml)	Absolute ethanol (ml)
Reaction control	0.0	10.4	0.32	1.28	22.3
Low reagent level	2.0	10.4	0.58	1.02	22.3
Medium reagent level	6.0	10.4	1.1	0.5	22.3
High reagent level	10.0	10.4	1.6	-	22.3

[a] Dry starch basis.
[b] Aqueous ethanol reaction system was based on 5.0 g (d.b.) starch granules.
[c] Final ethanol concentration in reaction medium: 65% (v/v) (Huber & BeMiller, 2001).
[d] Reaction medium pH = 11.5.

Table 2
Mean[a] molar substitution (MS) values for waxy and normal wheat starch A-type granules substituted with a propylene oxide analog (POA).

Starch Derivatives	POA (%, s.b.[b])	Molar substitution	
		Waxy starch granule	Normal starch granule
Low reagent level	2.0	0.002 ± 0.000	0.003 ± 0.000
Medium reagent level	6.0	0.012 ± 0.000	0.012 ± 0.000
High reagent level	10.0	0.024 ± 0.001	0.023 ± 0.000

[a] Mean values of two replicate reactions.
[b] Dry starch basis.

based on net sulfur levels (sulfur level of starch derivative minus sulfur level of reaction control), are depicted in Table 2.

2.4. Conversion of wheat starch POA derivatives to silver(I) salts

Substituted derivatives, which possessed anionic substituent groups (SO_3^-), were converted to silver(I) salts as outlined by Gray and BeMiller (2004) in preparation for viewing by reflectance confocal laser scanning microscopy (R-CLSM). All silver-exchange and wash procedures described below were conducted in the dark to protect the samples from exposure to light. Each starch derivative (0.5 g, d.b.) was combined with 0.25 M silver nitrate (35 ml) in a 50-ml centrifuge tube, following by shaking on a Wrist Action Shaker for 24 h. Starch derivatives in tubes were recovered by centrifugation (3000 × *g*, 15 min), and supernatants were carefully discarded. This silver-exchange process (consisting of the addition of silver nitrate solution, shaking for 24 h, and centrifugation for starch recovery) was repeated a total of three times for each starch derivative. Silver-exchanged starch derivatives were then washed twice with deionized water to remove unbound silver(I) cations from granules as follows. Silver-exchanged starch derivatives were re-suspended in deionized water (35 ml), shaken for 30 min on a Wrist Action Shaker, and recovered by centrifugation (3000 × *g*, 15 min); supernatants of both washes were carefully decanted/discarded. After washing, the silver-exchanged derivatives were re-suspended in 85% (v/v) aqueous ethanol, recovered on a Büchner funnel, and allowed to air-dry. Reaction controls were subjected to the same silver-exchange and wash schemes as defined for the modified starch products.

2.5. Reflectance confocal laser scanning microscopy (R-CLSM)

Small amounts of silver-exchanged starch derivatives were evenly dusted onto glass slides that had been lightly coated with wax, and slides were passed quickly over a flame to affix starch granules to the glass surface. Mounted starch specimens were exposed to UV light (254 nm, USG30T8, Bulbtronics Inc., Farmingdale, NY, USA) for 48 h to reduce silver(I) ions to silver atoms and/or atom clusters. Following UV irradiation, slides containing starch derivatives received 2–3 drops of aqueous sucrose solution (20%, w/v) to achieve a uniform refractive index throughout the starch granules, and were overlaid with glass cover slips prior to viewing with confocal laser scanning microscopy in the reflectance mode (R-CLSM) (Gray & BeMiller, 2004).

Optical sections of modified starch granules were obtained using a Zeiss LSM 510 CLSM system equipped with an inverted microscope and a 63 × DIC objective lens (Thornwood, NY, USA). The light source was an Argon laser (488 nm) operated at 30% power, while light reflected from specimens was detected through a LP 475 emission filter. An amplifier offset parameter was set to −0.3 to minimize background noise. Starch granules were optically sectioned at 0.5 or 1.0 μm thickness intervals to obtain serial cross-section images. Obtained images were processed using Zeiss LSM Image Examiner software.

2.6. Preparation of three dimensional (3D) anaglyph images

For construction of 3D images, optical cross-sections representing just the inner regions of the starch granule matrix were selected from the full range of serial cross-sectional images obtained by R-CLSM (Fig. 1). Select groups of optical sections were digitally stacked on the *y*-axis in maximum transparency mode using Zeiss LSM Image Examiner software; reconstructed 3D images consisted of 64 projections with a 9° angle difference.

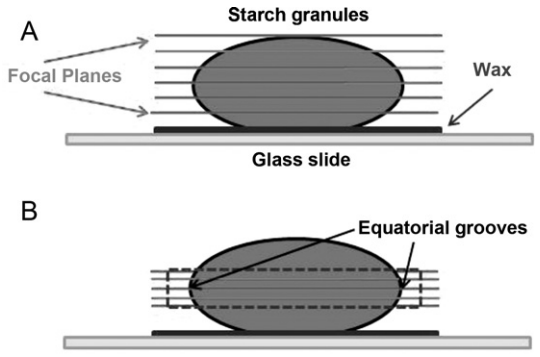

Fig. 1. Schematic diagram depicting, (A) a set of serial optical sections (slices) obtained at regular thickness intervals (focal planes) through a starch granule, and (B) a select series of optical cross-sections representing just the inner regions of the starch granule matrix (dotted line rectangle).

For creation of anaglyph images, selected cross-sectional images were reconstructed according to 3D image reconstruction parameters defined in the previous paragraph, and images were further colored red and green (or cyan). The green-colored 3D granule image was wrenched clockwise 7° against the *y*-axis of the red-colored 3D granule image, followed by digitally superimposing the twisted green-colored image onto the red-colored image. The anaglyph image provides stereoscopic 3D effects when viewed with 3D glasses fitted with red (left eye) and green (right eye) lens filters.

3. Results and discussion

3.1. Specimen preparation and R-CLSM optimization

Granular reaction patterns of substituted A-type granules of waxy and normal wheat starch were investigated using the scheme outlined by Gray and BeMiller (2004). This technique involves binding of silver(I) cations to anionic substituent groups (SO_3^-) of starch derivatives, followed by reduction of silver(I) cations to silver atoms via UV irradiation. Reaction locale is visualized via CLSM based on light reflected from silver atoms and/or atom clusters (bound at granular reaction sites). To reliably locate reaction sites within modified starch granules, it is necessary to effectively remove excess (unbound) silver(I) cations from silver-exchanged derivatives prior to treatment with UV irradiation (to eliminate the possibility of false positives).

Gray and BeMiller (2004) effectively removed excess silver(I) cations from granules by washing silver-exchanged starch derivatives with hot (≈65 °C) aqueous ethanol (85%, v/v), as previously described by Huber and BeMiller (2001). In applying this washing procedure within our study, virtually all POA derivatives experienced irreversible granule swelling, gelatinization and rupture. The temperature (≈65 °C) of the aqueous ethanol wash medium was destructive to the granule structures of wheat starch POA derivatives, which exhibited gelatinization onset and peak temperatures of approximately 55 and 65 °C, respectively (Kim & Huber, 2010a). The intra- and/or intermolecular repulsion of like-charged substituent groups covalently bound to starch molecules within granules led to partial or complete gelatinization of POA-derivatized starch granules during washing in hot 85% (v/v) aqueous ethanol. Consequently, the hot 85% (v/v) aqueous ethanol wash medium of Huber and BeMiller (2001) was not appropriate for removal of excess silver(I) cations from wheat starch POA derivatives.

Further study was devoted to establishing an appropriate method for removal of excess silver(I) cations from POA starch derivatives, wherewith granule integrity could be retained. Varying concentrations (50–85%, v/v) of aqueous ethanol used in conjunction with a variety of wash medium temperatures (<50 °C) proved unsuccessful. A 50% (v/v) aqueous ethanol wash medium employed at 40 °C was unable to remove unbound silver(I) cations from unmodified POA reaction controls (Fig. 2A). In contrast, the same unmodified POA reaction control, when washed with deionized water at ambient temperature (≈22 °C), exhibited a much reduced reflected light signal from granules (Fig. 2B), indicating that the majority of unbound silver(I) ions had been removed from granules. Using a deionized water wash medium (≈22 °C), no perceived irreversible granule swelling and only a very minimal amount of starch leaching from granules (0.02–0.05%, s.b.) was observed for POA starch derivatives during washing. Thus, deionized water appeared to be an appropriate and effective wash medium for removal of unbound silver(I) cations from silver-exchanged POA reaction controls and derivatives of waxy and normal wheat starch.

Though the deionized water medium removed the majority of excess silver(I) cations from granules of starch reaction controls,

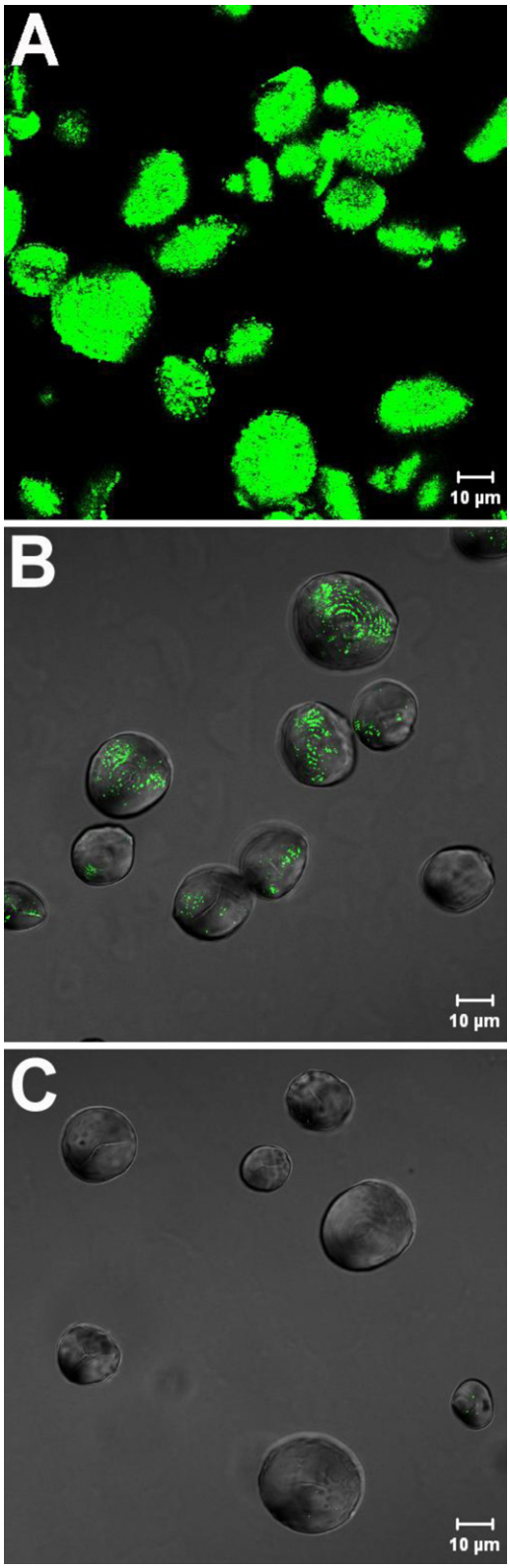

Fig. 2. R-CLSM optical cross-sections of waxy wheat starch A-type granules (reaction control) treated with 0.25 M silver nitrate, followed by washing with, (A) 50% (v/v) aqueous ethanol at 40 °C, (B) deionized water at ambient temperature, or (C) deionized water at ambient temperature in conjunction with adjustment of microscope parameters (detector gain, offset) to reduce background signal (scale bars = 10 μm).

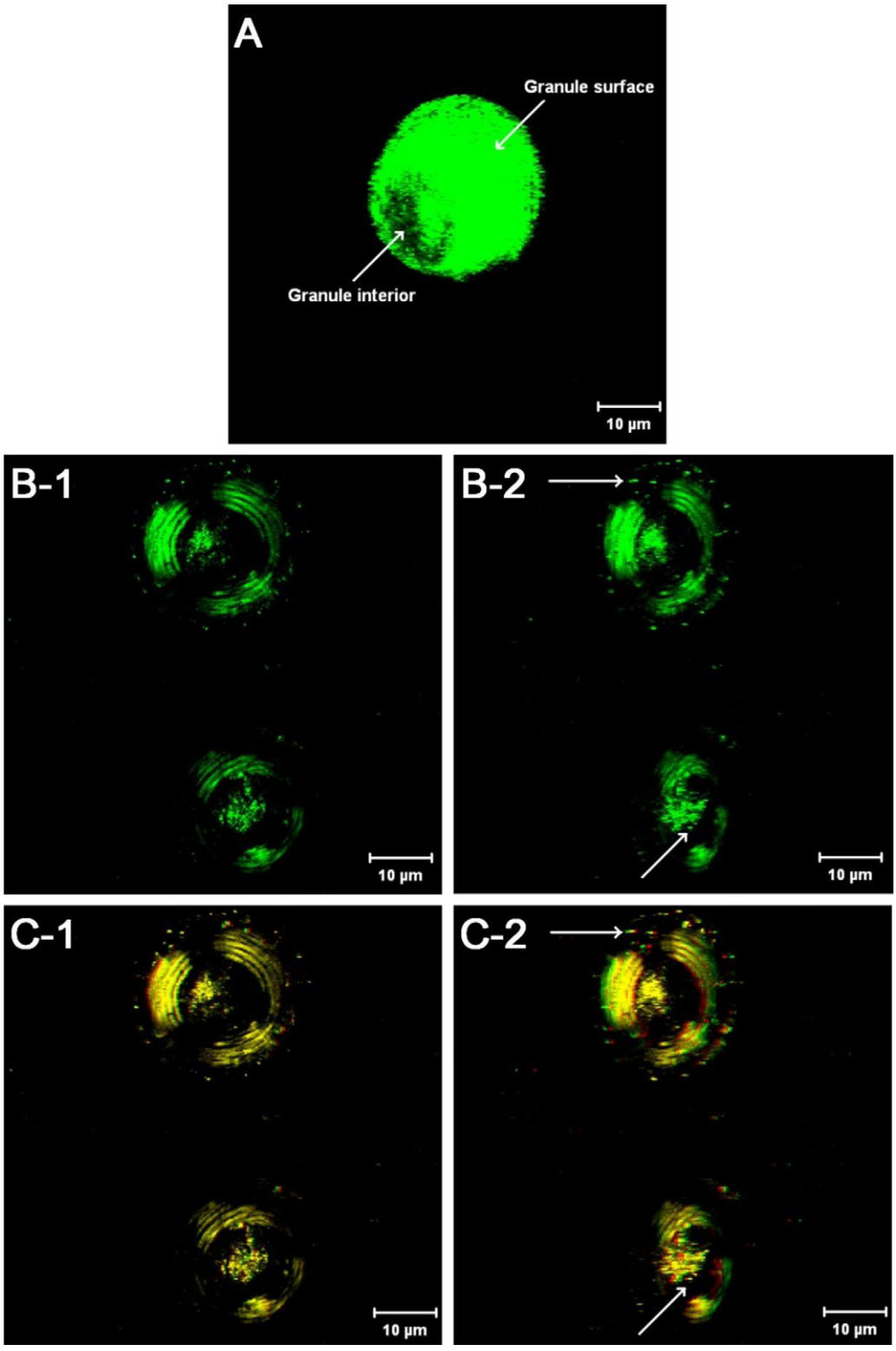

Fig. 3. Reconstructed 3D R-CLSM images of waxy wheat starch A-type granules derivatized with POA (2%, s.b.) representing, (A) all serial sections comprising a starch granule (refer to Fig. 1A), (B) select serial sections comprising the inner regions of the starch granule matrix (refer to Fig. 1B), or (C) the anaglyphic representation of Fig. 3B. Both, (B-1 and C-1) standard (normal front-facing), and (B-2 and C-2) partial side (slightly rotated) views of granules are presented for added perspective (scale bars = 10 μm). For visualization of images C-1 and C-2 in 3D, the reader is referred to the web version of the article for access to full color images that require 3D glasses (red and green lenses on left and right eyes, respectively).

some residual silver(I) cations still remained within the granules (Fig. 2B). To establish whether the residual silver atoms within granules of the unmodified reaction controls resulted from insufficient washing of unbound silver(I) cations, a silver-exchanged reaction control (i.e., waxy starch) was subjected to five additional wash cycles (beyond the two cycles normally used in the present study). No significant decrease in either the reflected signal intensity or pattern, due to the residual silver within granules, was

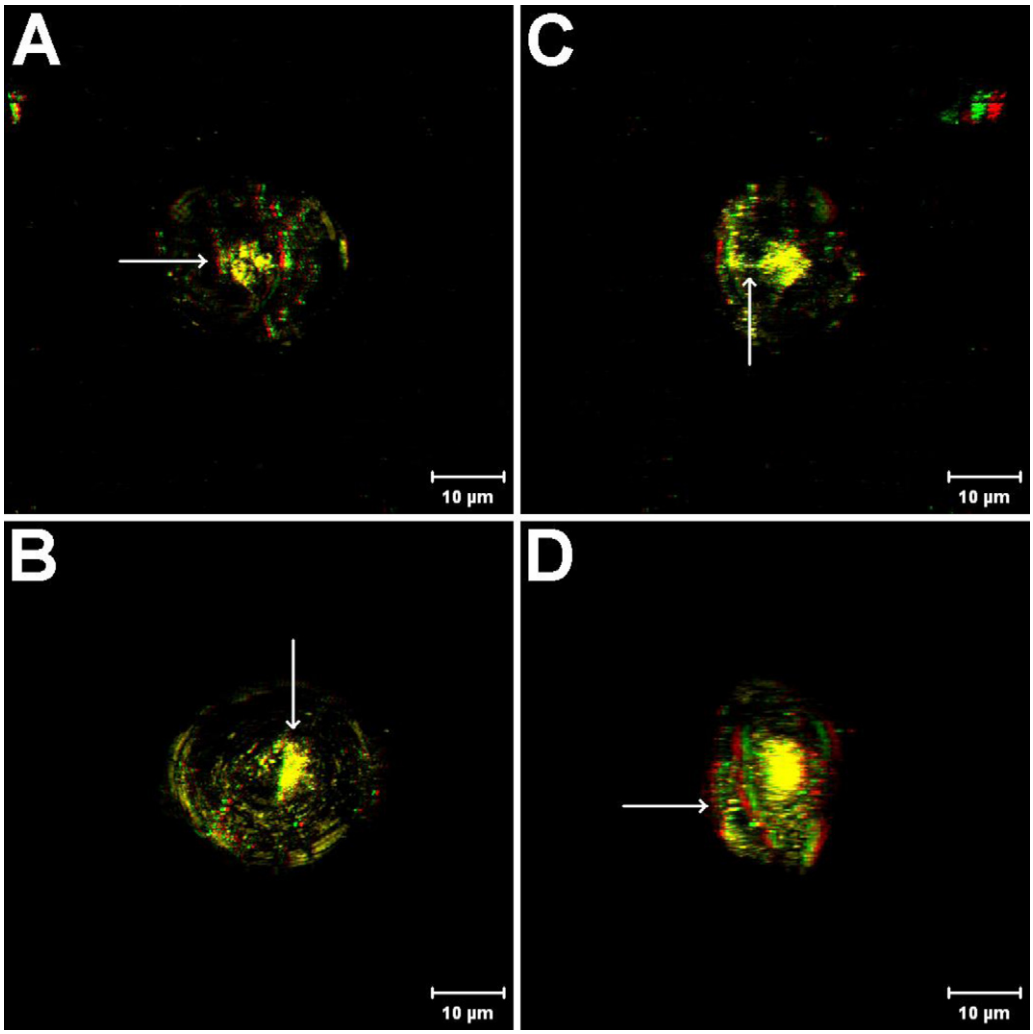

Fig. 4. Anaglyphic images representing, (A and B) standard, and (C and D) partial side views of, (A and C) waxy, and (B and D) normal wheat starch A-type granules derivatized with a low level of POA (Table 1; Molar substitution, MS = 0.0023 and 0.0028 for waxy and normal starch granules, respectively) (scale bars = 10 μm). For visualization of images in 3D, the reader is referred to the web version of the article for access to full color images that require 3D glasses (red and green lenses on left and right eyes, respectively).

observed over the course of extended washing (data not shown). The background signal caused by the presence of residual silver atoms after exhaustive washing appeared to be due to the binding of silver ions by trace anionic components within the granules (e.g., lysophospholipids, starch granule-associated proteins). Gray and BeMiller (2004) reported the same phenomenon in their experiments with corn, potato and sorghum starch substrates. Nevertheless, this unwanted signal contributed background noise to R-CLSM images, and had potential to interfere with or even compromise visualization of granular reaction patterns within modified starch derivatives.

To eliminate and/or minimize the background noise, microscope conditions were optimized using unmodified reaction controls, which had been subjected to the complete R-CLSM specimen preparation protocol (i.e., silver cation exchange, washing with deionized water at ambient temperature, and reduction of silver(I) ions to silver atoms by UV irradiation). Optimization was achieved by manually manipulating microscope parameters (e.g., detector gain, offset) to reduce the background signal in the reaction control specimen. Microscope conditions for each derivative/genotype combination were individually optimized using its own respective reaction control, and were held constant while viewing all specimens of a common derivative/genotype series. Using the optimized microscope conditions, the background noise was very effectively minimized in granules of the various reaction control starches (Fig. 2C), though some very weak (minor) background signals were infrequently observed in a minority of granules. Using the noted microscope parameter adjustments (developed using the unmodified reaction control starches), R-CLSM images of the modified starch granule derivatives generated under optimized microscope conditions more effectively highlighted true granular reaction sites, and depicted valid granular reaction patterns.

Nevertheless, it is necessary to point out that granular reaction patterns visualized in this study might not reveal all possible reaction sites within derivatized starch granules. This limitation results from the fact that: (1) it is not known whether the degree of resolution possible with R-CLSM is be capable of resolving a single silver atom or reaction site (but might require clusters of silver atoms, representing multiple reaction sites, for detection) (Gray & BeMiller, 2004), and (2) a slight reduction in R-CLSM gain was required to eliminate background noise within reaction controls (could slightly reduce overall sensitivity in determining granular reaction patterns of starch derivatives). Despite the noted limitations, the R-CLSM method utilized here provides a valid and useful approach for visualizing the predominant granular locale of

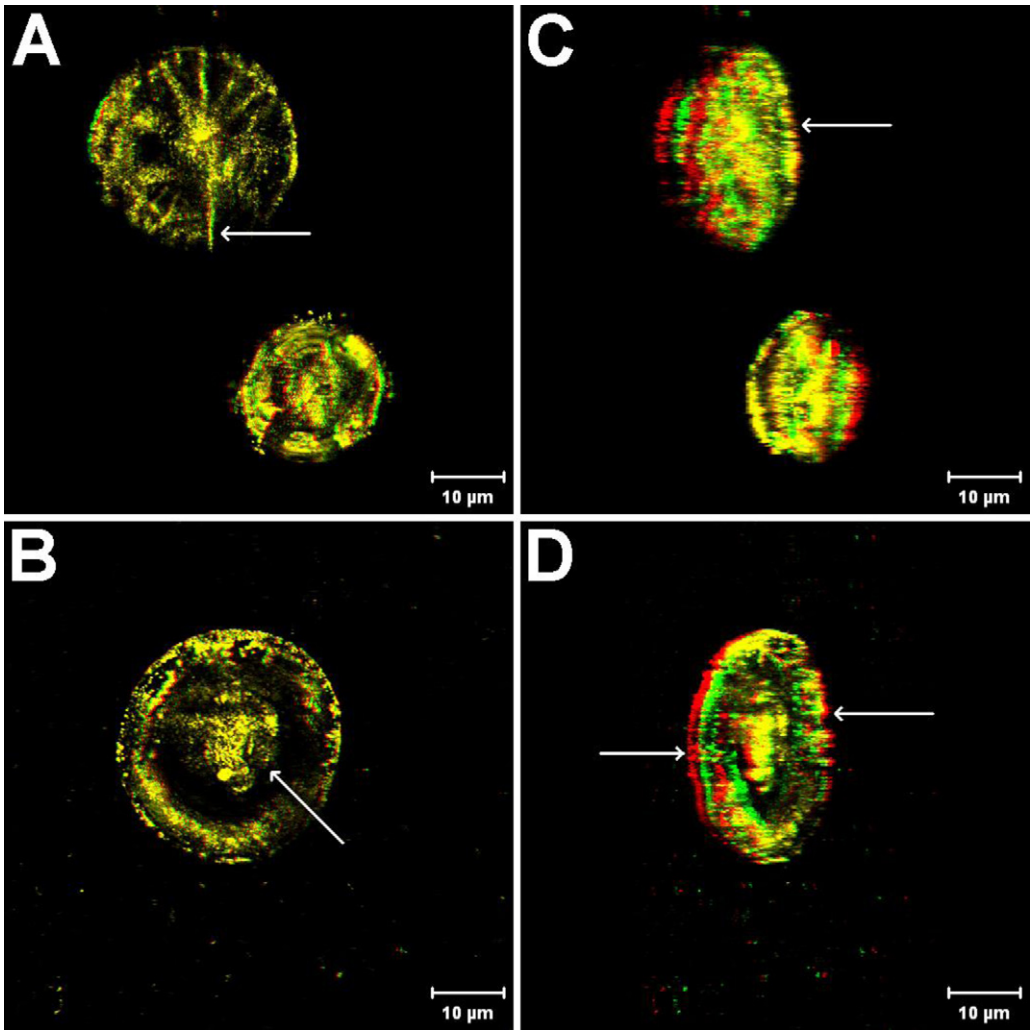

Fig. 5. Anaglyphic images representing, (A and B) standard, and (C and D) partial side views of, (A and C) waxy, and (B and D) normal wheat starch A-type granules derivatized with a medium level of POA (Table 1; MS = 0.0124 and 0.0119 for waxy and normal starch granules, respectively) (scale bars = 10 μm). For visualization of images in 3D, the reader is referred to the web version of the article for access to full color images that require 3D glasses (red and green lenses on left and right eyes, respectively).

reaction and for elucidating paths of reagent flow within modified starch granules.

3.2. Three dimensional (3D) and anaglyph imaging of granular reaction patterns

Gray and BeMiller (2004) presented individual optical sections from the central regions of derivatized corn and potato starch granules to elucidate the locale of reaction sites within granules. In our study, however, it was not always possible to select a single representative optical section (from a set of serial cross-sections) that fully depicted the composite granular reaction pattern, as reaction patterns of individual serial sections differed slightly depending on their granular origin.

To provide a more comprehensive view of granular reaction patterns, serial cross-sections (obtained via CLSM; Fig. 1A) of substituted starch granules were reconstructed into three-dimensional (3D) images. For constructed 3D images of POA starch derivatives at even the lowest derivatization level (2% POA, s.b.) (Fig. 3A), high intensities of reflection were observed throughout the granules, but more particularly from granule surfaces. Gray and BeMiller (2004) likewise reported heavy reaction at external granule surfaces of POA- and $POCl_3$-derivatized starches (corn, sorghum, potato) viewed by R-CLSM. This same challenge was encountered for constructed 3D images of all starch derivatives, regardless of the reagent addition level (images not shown). Thus, it was not possible to discern differences in either the degree or pattern of reaction within granule interiors (which were of primary interest in this study) due to the high extent of reaction at or near granule surfaces.

For viewing reaction patterns within the granule matrix, 3D images were constructed using only a limited number of serial cross-sections encompassing exclusively the internal granule regions of A-type granules (Fig. 1B) comprising the granule equatorial groove (image thickness ~3–5 μm). Examples illustrating both the standard and slightly rotated side views of the same 3D image are provided in Fig. 3B-1 and B-2, respectively. The standard view (Fig. 3B-1) of the 3D granule image depicts reaction within the concentric ring structures of granules and also as short tiny dots or clusters in the peripheral regions of granules. The partial side view of the same 3D image (Fig. 3B-2, simply a slightly rotated view of the image depicted in Fig. 3B-1) depicts the tiny dots observed in the standard view of the 3D image as short lines or streaks, likely representing short channels penetrating into the granule matrix from the granule surface. Thus, the adapted 3D images of exclusively the inner granular regions provided a more discerning perspective of granular reaction patterns within granules compared to either individual cross-sections or 3D images of entire granules (constructed

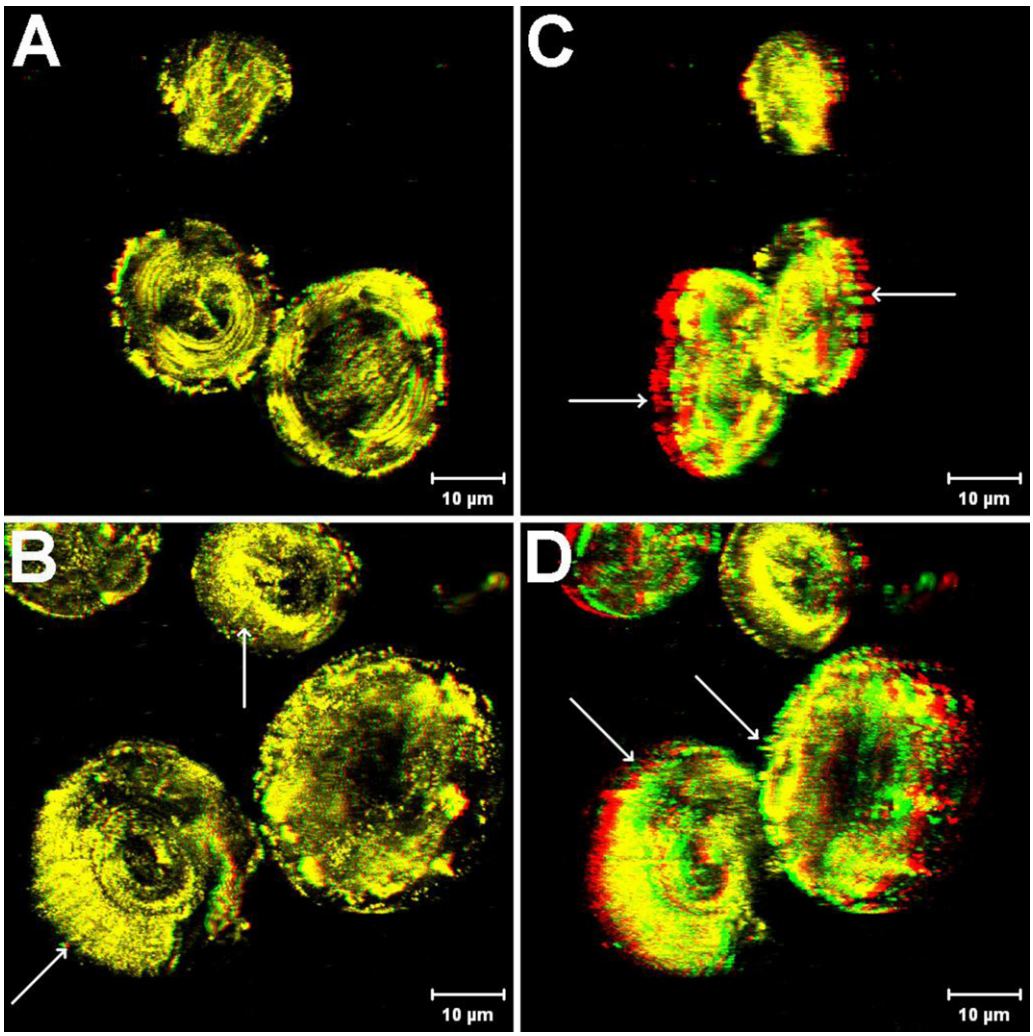

Fig. 6. Anaglyphic images representing, (A and B) standard, and (C and D) partial side views of, (A and C) waxy, and (B and D) normal wheat starch A-type granules derivatized with a high level of POA (Table 1; MS = 0.0235 and 0.0230 for waxy and normal starch granules, respectively) (scale bars = 10 μm). For visualization of images in 3D, the reader is referred to the web version of the article for access to full color images that require 3D glasses (red and green lenses on left and right eyes, respectively).

from all serial sections of a granule). Nevertheless, these 3D images (Fig. 3B-1 and B-2) of inner granular regions still suffered from the limitation of being depicted as 2D (flat) images, which did not allow full differentiation of topography within granules.

This shortcoming was overcome by creating anaglyph images, which provided stereoscopic 3D effects with the aid of 3D glasses. Anaglyphic images reconstructed from the same set of serial cross-sections previously used to construct the 3D images (Fig. 3B-1 and B-2) are provided in Fig. 3C-1 and C-2 for comparison. In the standard view (Fig. 3C-1) of the anaglyphic image, the true topography of the tiny dots or dot clusters, which were elevated to varying depths above the highlighted concentric ring structures, could be visualized, in contrast to the standard 3D image (Fig. 3B-1), where the entire signal was depicted within a single flat 2D plane. In the partial side view of the anaglyph image (Fig. 3C-2, simply the slightly rotated view of the same image depicted in Fig. 3C-1), it became clear that the tiny dots (observed in Fig. 3C-1) were actually cross-sections of short channels penetrating toward the granule interior from the granule surfaces (Fig. 3C-1, noted by arrows). The partial side view (Fig. 3C-2) of the anaglyphic granule image further clarified that the highlighted concentric ring structures were confined to the equatorial groove regions of the granule matrix. Thus, because of the enhanced perspective provided, anaglyphic granule images were used to investigate internal reaction patterns within wheat starch A-type granules for all starch derivatives of the study.

3.3. Reaction patterns of POA derivatives of waxy and normal wheat starch A-type granules

Granular reaction patterns of POA-derivatized wheat starch A-type granules were tracked across three reagent addition levels, providing variable levels of MS for each genotype (Table 2). Because microscope settings and the level of digital zoom (2×) were held constant for all modification levels of a given starch genotype, signal intensity differences between images representing the various modification levels of the study are attributable to actual differences in the relative concentrations of silver atoms and/or atom clusters within granules, reflecting true differences in degree of derivatization. However, it was not possible to directly compare signal intensities of granular reaction patterns across genotypes, as microscope conditions for viewing granular reaction patterns were individually optimized for each starch genotype. In general, an increase in reagent addition level increased homogeneity of reaction for all derivatives, with granular reaction pattern details discussed below in the order of increasing reagent addition levels.

Anaglyphic images for POA-derivatized A-type granules of waxy and normal wheat starch are depicted in Figs. 4–6, corresponding to low (2%), medium (6%), and high (10%) POA substitution levels, respectively. Overall, observed granular reaction patterns for POA derivatization did not differ between waxy and normal wheat starches. For the low level of POA substitution, central granule regions (e.g., cavities) were most heavily highlighted or reacted (reagent effectively reached granule central regions even at low addition levels), though minimal reaction was generally observed within the granule matrix (Fig. 4A and B). Partial side (rotated) views (Fig. 4C and D) also revealed fine channels connecting the highlighted granule hilum region to the external granule surface, as well as the presence of short channels, penetrating inward into the granule matrix from varying directions. These results suggest that reagent reached the granule hilum region rather rapidly through channels, which connect the inner regions of granules to the extra-granular environment and provide granular access to reagent.

For the medium POA substitution level, intense reaction continued within the central granule region, around cavities, and within the granule matrix near channels (Fig. 5). Multiple channel structures within granules were visualized originating from external granule surfaces of the equatorial groove region (Fig. 5A) and from other surfaces of granules at random (Fig. 5C and D). Perceived boundaries of channel structures within granules appeared to broaden or enlarge as reagent diffused from channels into the granule matrix. The predominant path of POA flow into the granule matrix occurred via lateral diffusion at channel surfaces. Though reagent was able to access the granule hilum region of granules via channels for even the lowest level of POA addition (Fig. 4), an inside-out pattern of reagent flow from inner cavity surfaces outward toward external granule surfaces was less prevalent in wheat starch granules than previously reported for corn starch granules reacted with the same reagent (Gray & BeMiller, 2004; Huber & BeMiller, 1997, 2001). At the highest POA substitution level, reactions became increasingly homogeneous throughout the granule matrix (Fig. 6), though some variation was observed amongst granules. Channel boundaries became much less discernable as reaction homogeneity increased, and reagent flow continued from channels surfaces into the granule matrix (Fig. 6 arrows), whereas concentric rings within granules became clearly visible, most likely due to the differential reaction of starch chains associated with amorphous versus semi-crystalline growth rings, providing evidence that reaction was not completely homogeneous. This observation parallels that of Chen, Schols, and Voragen (2004), who concluded that substitution of potato and sweet potato starches with acetic anhydride occurred mainly within amorphous regions and only in the outer lamellae of crystalline regions. However, the progression of reaction from the external granule surfaces into the granule matrix was not observed, even though derivatization was heavy at the external granule surfaces, as previously reported for waxy maize starch by both Huber and BeMiller (2001) and Gray and BeMiller (2004).

Maximum POA MS levels in this study were limited due to the intermolecular strain imposed on granules by addition of charged substituent groups to starch chains (higher MS values resulted in gelatinization during reaction). In extrapolating to industrial modification levels, an even greater degree of reaction homogeneity within granules would be expected for commercial hydroxypropylated starches (MS ≈ 0.1–0.2) relative to those of this study (MS ≈ 0.025).

Acknowledgement

We acknowledge the National Research Initiative of the USDA Cooperative State Research, Education and Extension Service for financial support of this study (grant no. 2004-35503-14128).

References

AACC. (2000). *Approved methods of the American Association of Cereal Chemists (AACC), method 26–31* (10th ed.). St. Paul: AACC International.

Alexander, R. J. (1992). Carbohydrates used as fat replacers. In R. J. Alexander, & H. F. Zobel (Eds.), *Developments in carbohydrate chemistry* (pp. 343–370). St. Paul: American Association of Cereal Chemistry.

BeMiller, J. N. (1997). Starch modification: Challenges and prospects. *Starch/Stärke*, *49*, 127–131.

Chen, Z., Schols, H. A., & Voragen, A. G. J. (2004). Differently sized granules from acetylated potato and sweet potato starches differ in the actyl substitution pattern of their amylose populations. *Carbohydrate Polymers*, *56*, 219–220.

Geera, B. P., Nelson, J. E., Souza, E., & Huber, K. C. (2006). Granule bound starch synthase I (GBSSI) gene effects related to soft wheat flour/starch characteristics and properties. *Cereal Chemistry*, *83*, 544–550.

Gray, J. A., & BeMiller, J. N. (2004). Development and utilization of reflectance confocal laser scanning microscopy to locate reaction sites in modified starch granules. *Cereal Chemistry*, *81*, 278–286.

Gray, J. A., & BeMiller, J. N. (2005). Influence of reaction conditions on the location of reactions in waxy maize starch granules reacted with a propylene oxide analog at low substitution levels. *Carbohydrate Polymers*, *60*, 147–162.

Han, J.-A., & BeMiller, J. N. (2005). Rate of hydroxypropylation of starches as a function of reaction time. *Starch/Stärke*, *57*, 395–404.

Han, J.-A., & BeMiller, J. N. (2006). Influence of reaction conditions on MS values and physical properties of waxy maize starch derivatized by reaction with propylene oxide. *Carbohydrate Polymers*, *64*, 158–162.

Han, J.-A., & BeMiller, J. N. (2007). Preparation and physical characteristics of slowly digesting modified food starches. *Carbohydrate Polymers*, *67*, 366–374.

Huber, K. C., & BeMiller, J. N. (1997). Visualization of channels and cavities of corn and sorghum starch granules. *Cereal Chemistry*, *74*, 537–541.

Huber, K. C., & BeMiller, J. N. (2000). Channels of maize and sorghum starch granules. *Carbohydrate Polymers*, *41*, 269–276.

Huber, K. C., & BeMiller, J. N. (2001). Location of sites of reaction within starch granules. *Cereal Chemistry*, *78*, 173–180.

Kavitha, R., & BeMiller, J. N. (1998). Characterization of hydroxypropylated potato starch. *Carbohydrate Polymers*, *37*, 115–121.

Kim, H.-S., & Huber, K. C. (2008). Channels within soft wheat starch A- and B-type granules. *Journal of Cereal Science*, *48*, 159–172.

Kim, H.-S., & Huber, K. C. (2010a). Impact of A/B-type granule ratio on reactivity, swelling, gelatinization, and pasting properties of modified wheat starch. Part I: Hydroxypropylation. *Carbohydrate Polymers*, *80*, 94–104.

Kim, H.-S., & Huber, K. C. (2010b). Physicochemical properties and amylopectin fine structures of A- and B-type granules of waxy and normal soft wheat starch. *Journal of Cereal Science*, *51*, 256–264.

Shi, X., & BeMiller, J. N. (2000). Effect of sulfate and citrate salts on derivatization of amylose and amylopectin during hydroxypropylation of corn starch. *Carbohydrate Polymers*, *43*, 333–336.

Singh, J., Kaur, L., & McCarthy, O. J. (2007). Factors influencing the physico-chemical, morphological, thermal and rheological properties of some chemically modified starches for food applications – A review. *Food Hydrocolloids*, *21*, 1–22.

Tester, R. F., Karkalas, J., & Qi, X. (2004). Starch-composition, fine structure and architecture. *Journal of Cereal Science*, *39*, 151–165.

Woo, K., & Seib, P. A. (1997). Cross-linking of wheat starch and hydroxypropylated wheat starch in alkaline slurry with sodium trimetaphosphate. *Carbohydrate Polymers*, *33*, 263–271.

Woo, K., & Seib, P. A. (2002). Cross-linked resistant starch: Preparation and properties. *Cereal Chemistry*, *79*, 819–825.

Wurzburg, O. B. (2006). Modified starches. In A. M. Stephen, G. O. Phillips, & P. A. Williams (Eds.), *Food polysaccharides and their applications* (2nd ed., pp. 25–85). Boca Raton: CRC Press.

Zobel, H. F., & Stephen, A. M. (2006). Starch: Structure, analysis, and application. In A. M. Stephen, G. O. Phillips, & P. A. Williams (Eds.), *Food polysaccharides and their applications* (2nd ed., pp. 25–85). Boca Raton: CRC Press.